# A chemical approach towards the photosynthetic reaction center

Atsuhiro Osuka,[a] Noboru Mataga[b] and Tadashi Okada[c]

*[a]Division of Chemistry, Graduate School of Science, Kyoto University, Sakyo-ku, Kyoto 606-01, Japan*
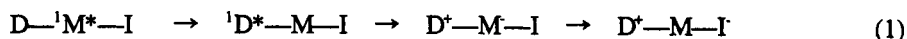*[b]Institute for Laser Technology, Nishiku, Osaka 550, Japan*
*[c]Department of Chemistry, Faculty of Engineering Science, Osaka University, Toyonaka 560, Japan*

*Abstract.* Phenylene-bridged zinc diporphyrin (D)—monoporphyrin (M)—pyromellitimide (I) triads were prepared as models for the photosynthetic reaction center (RC). With D and I fixed, the central monoporphyrin subunit is tuned from octaalkyl-substituted zinc porphyrin ($M_0$) to a doubly strapped metal-free porphyrin (SH), a β-unsubstituted metal-free porphyrin (H), and a β-unsubstituted zinc porphyrin (Z) in order to achieve a RC-type sequential ET relay. In D—$M_0$—I and D—SH—I, the charge separation (CS) between $^1M_0^*$ and I or $^1SH^*$ and I and a subsequent hole transfer to D provide $D^+$—$M_0$—$I^-$ and $D^+$—SH—$I^-$, respectively. Upon excitation of D—H—I, an effective CS between the porphyrin pigments provides $D^+$—$H^-$—I which is converted to $D^+$—H—$I^-$ by a subsequent charge shift reaction in 0.8 overall quantum yield in a manner analogous to that in RC. D—Z—I gives $D^+$—Z—$I^-$ in 0.4 overall quantum yield both in DMF and THF but the transient absorption spectra revealed that a stepwise ET relay of $^1D^*$—Z—I → $D^+$—$Z^-$—I →$D^+$—Z—$I^-$ in DMF, while superexchange mediated long-distance electron transfer is suggested in THF.

## INTRODUCTION

The appearance of the X-ray structure of bacterial photosynthetic reaction center (RC) has exerted a great impact on mechanistic studies of this natural charge separation (CS) apparatus (ref. 1). In the RC, light energy captured by photosynthetic pigments is effectively collected at the special pair (SP), giving $^1(SP)^*$ as the final energy sink as well as the first electron donor. Subsequent electron-transfer (ET) relay over cofactors such as bacteriochlorophyll, bacteriopheophytin, $Q_a$, and $Q_b$ results in a quantitative transmembrane CS. During the last decade, structurally well defined synthetic models have proven to be particularly effective in understanding the mechanism of these biological ET reactions (ref. 2). One of the long-standing issues of these model studies is the achievement of the sequential photochemical events in RC. Here we present our efforts exploring synthetic triads D—M—I, where D, M, and I represent a 1,2-phenylene-bridged zinc porphyrin dimer, a porphyrin monomer, and a pyromellitimide electron-acceptor, respectively. The first goal we set is the achievement of the following photochemical reactions (eq. 1); the singlet excitation energy captured by D and M is initially collected at D, and the initial CS between $^1D^*$ and M is accompanied by a charge shift reaction (CSH) to give $D^+$—M—$I^-$ as a secondary, long-lived ion-pair state. Functionally, D, M, and I may correspond to SP, bacteriopheophytin, and $Q_a$, respectively. Here it may be pointed out that the analysis and molecular design are quite simple but it has been very difficult to achieve all these photochemical events within a single synthetic molecule. Although there have been a lot of synthetic triads consisting of electron donor (EA) )—porphyrin (P)—electron acceptor (EA) which provide long-lived charge separated states by a sequential ET relay of eq. 2 (ref. 2, 3), this sequence is different from that in the RC.

$$D—^1M^*—I \quad → \quad ^1D^*—M—I \quad → \quad D^+—M—I \quad → \quad D^+—M—I^- \qquad (1)$$

$$ED—^1P^*—EA. \quad → \quad ED—P^+—EA^- \quad → \quad ED^+—P—EA^- \qquad (2)$$

## MOLECULAR DESIGN

In comparison to $M_0$, the D moiety has lower $S_1$-energy by 0.19 eV and lower oxidation potential by 0.24 V (ref. 4). These differences are quite analogous to those found for a monomeric bacteriochlorophyll and SP, thereby encouraging the use of D as a functional model of SP. We used I as an electron acceptor, since it is chemically stable and has a pertinent reduction potential, and once reduced it exhibits a characteristically intense and sharp absorption band around 715 nm which is very useful in tracing ET dynamics of complicated molecular systems (ref. 5). Here we summarize the excited-state dynamics of four synthetic triads D—M—I. With the D and I moieties fixed in the series, the central M moiety is changed from original zinc porphyrin monomer ($M_0$) to a doubly-strapped metal-free porphyrin (SH), a β-unsubstituted metal-free porphyrin (H), and a β-unsubstituted zinc porphyrin (Z) in pursuit of achieving a RC-type sequential ET relay. We will discuss the excited-state dynamics of these models observed mostly in THF except the cases where significant changes in the ET dynamics are observed upon the change of the solvent polarity.
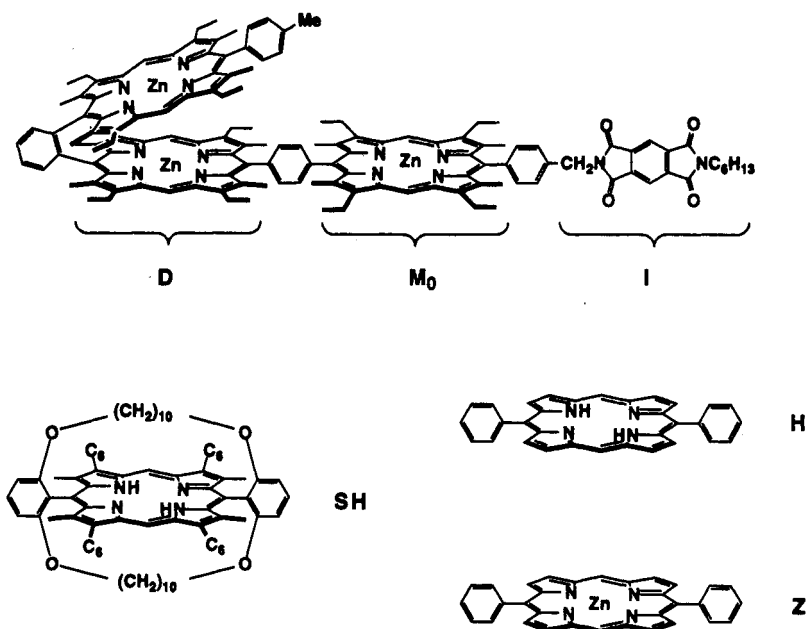


## RESULTS AND DISCUSSION

**D—$M_0$—I** The absorption spectrum of D—$M_0$—I is roughly a simple sum of the absorption spectra of D and $M_0$. Both the D and $M_0$ moieties are excited by irradiation at 532 nm, while irradiation at 620 nm leads to selective excitation of the D moiety. The former excitation leads to population of $^1$D*—$M_0$—I (1.97 eV) and D—$^1M_0$*—I (2.16 eV) which is followed by singlet-singlet energy transfer ($2.0 \times 10^{11}$ s$^{-1}$) from $M_0$ to D. This energy transfer has been clearly detected by the fluorescence lifetime measurement and the transient absorption spectroscopy. In competition with this efficient energy transfer, CS between $^1M_0$* and I is accompanied by a hole transfer to provide D$^+$—$M_0$—I$^-$ in 0.05 overall quantum yield (ref. 5). On the other hand, the selective excitation of D (at 620 nm) does not lead to formation of charge separated states, i.e. the lifetime and decay behavior of $^1$D*—$M_0$—I are exactly the same as those of the reference $^1$D* alone. Thus, the D subunit in this model acts as an efficient singlet energy sink but as a poor electron donor towards the $M_0$ subunit, thereby reducing the overall CS quantum yield. In line with these results, the energy levels of the ion pair states are estimated on the basis of the redox potentials as follows; D$^+$—$M_0^-$—I (2.20 eV), D—$M_0^+$—I$^-$ (1.56 eV), and D$^+$—$M_0$—I$^-$ (1.48 eV). Detailed analysis of the transient absorption spectra revealed the ET rate constants as follows; $1.6 \times 10^{10}$ s$^{-1}$ for D—$^1M_0$*—I → D—$M_0^+$—I$^-$, $1.9 \times 10^{10}$ s$^{-1}$ for D—$M_0^+$—I$^-$ → D$^+$—$M_0$—I$^-$, $9.5 \times 10^9$ s$^{-1}$ for D—$M_0^+$—I$^-$ → D—$M_0$—I, respectively. D$^+$—$M_0$—I$^-$ has a lifetime of 260 ns and has been detected by time-resolved ESR experiments (ref. 6).
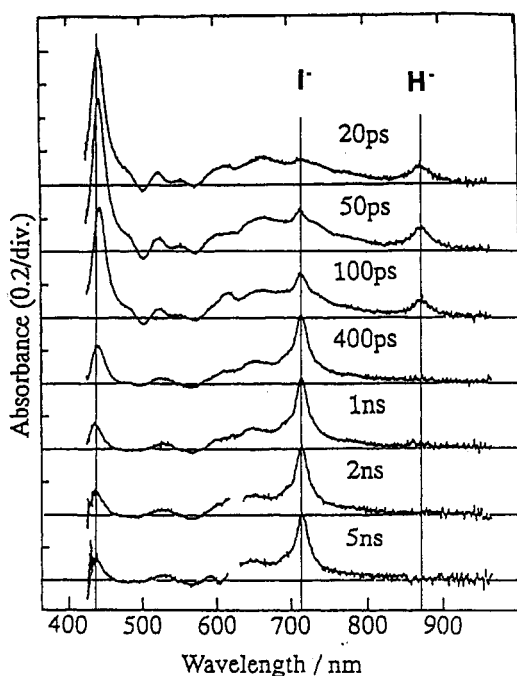
Fig. 1 Transient expression spectra of a $1 \times 10^{-4}$ M solution of D—H—I in THF excited with 8 ps, 618 nm pulses.

Lack of ET-reactivity in $^1$D*—$M_0$—I can be ascribed to an unfavorable energy diagram that D$^+$—$M_0^-$—I is higher in energy than $^1$D*—$M_0$—I. It is to be noted that the reaction sequence (eq. 3) leading to the formation of D$^+$—$M_0$—I$^-$ is analogous to eq. 2, being different from the reaction sequence in RC. We also prepared D—$M_0$—I—quinone (Q) tetrads (ref. 7), which provide D$^+$—$M_0$—I—Q$^-$ with 1.6-2.6 µs lifetime.

$$D—{}^1M^*—I \;\rightarrow\; D—M_0{}^+—I^- \;\rightarrow\; D^+—M_0—I^- \tag{3}$$
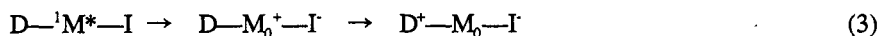
**D—SH—I** Usually metal-free porphyrin has a lower reduction potential compared with the corresponding zinc porphyrin. Thus, we attempted to prepare D—metal free porphyrin—I triad with intention to induce CS between D and a porphyrin monomer upon irradiation. It is worthy to note that the molecular composition of D—SH—I is quite analogous to RC. From a synthetic point of view, separation of desired partially metallated compounds from other metallated species was thought to be very difficult. These difficulties were overcome by introducing double straps over the metal-free porphyrin which prevented the metallation there. Indeed, simple heating of an all metal-free precursor in the presence of $Zn(OAc)_2$ gave D—SH—I in a quantitative yield (ref. 8). The energy levels of key states are as follows; $^1$D* (1.97 eV), $^1$SH* (1.95 eV), D$^+$—SH$^-$—I (1.82 eV), D—SH$^+$—I$^-$ (1.82 eV), and D$^+$—SH—I$^-$ (1.48 eV). Although the energy level of D$^+$—SH$^-$ ion pair seems to be lower than those of the excited states, we did not observe the formation of such a state upon irradiation of D—SH nor D—SH—I. Since $^1$D* and $^1$SH* have similar excitation energies, there is an equilibrium of $^1$D*—SH ⇌ D—$^1$SH* which is attained within ca. 50 ps. The secondary ion pair D$^+$—SH—I$^-$ is formed relatively slowly with a time constant of ca. 700-800 ps and its concentration becomes constant in a ns-time range. The overall quantum yield for the formation of D$^+$—SH—I$^-$ is 0.26. The $^1$SH*—I moiety undergoes intramolecular CS to give SH$^+$—I$^-$ with a rate constant of $1.0 \times 10^9$ s$^{-1}$, and subsequent charge recombination (CR) to the ground state with a rate constant of ca. $1 \times 10^{10}$ s$^{-1}$. Thus we consider that the similar ET reactions proceed in D—SH—I to give D—SH$^+$—I$^-$ in which a hole transfer provides D$^+$—SH—I$^-$ in competition with the rapid CR reaction. This reaction sequence is again analogous to eqs. 2 and 3. Another interesting finding is a remarkable long lifetime (12 µs) of D$^+$—SH—I$^-$ that is ca. 50-times longer than the lifetime of D$^+$—$M_0$—I$^-$. Through systematic studies on a series of the related triads, we found that the temperature dependence of the rates of CR reaction of triad ion pair state (D$^+$—M—I$^-$) to their ground state (D—M—I) are usually very small except the case of D$^+$—SH—I$^-$, which displays biphasic temperature dependence consisting of a distinctly temperature-dependent region and a virtually temperature-independent region. Given that the temperature-independent behavior to be stemming from predominance of strong electron coupling given by superexchange interactions with the central monomer subunit as virtual states, the observed temperature-

dependent region may correspond to a stepwise backward ET sequence of endothermic $D^+$—SH—$I^- \rightarrow$ $D^+$—SH$^-$—I or D—SH$^+$—$I^-$ followed by a highly exothermic CR to the ground state D—SH—I. The first step is energetically uphill by ca. 0.34 eV, thus making the overall charge recombination temperature dependent. We also prepared D—$M_0$—SH—I tetrad and examined its excited state dynamics. Formally this tetrad well duplicates the molecular composition of the ET-active L-branch in RC. $D^+$—$M_0$—SH—$I^-$ ion pair was indeed generated in ca. 0.2 overall yield and its lifetime is 16 μs (ref. 8).
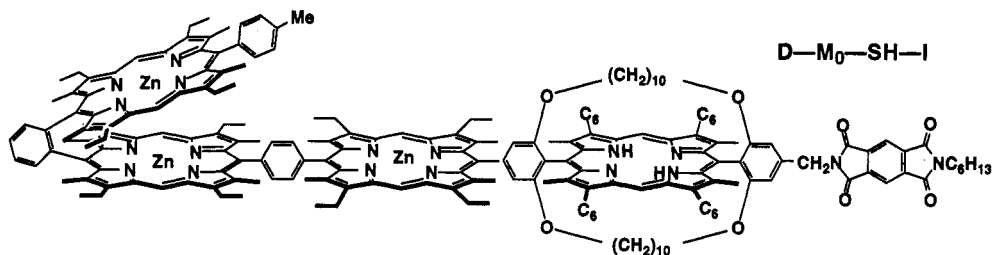


**D—H—I** Here the central monomer subunit is a β-unsubstituted metal-free porphyrin (H), in which electron donating β-alkyl substituents are all omitted, thus making this unit easier to be reduced and harder to be oxidized in comparison to $M_0$ and SH. Fortunately, this molecule was prepared by selective metallation only at the diporphyrin site (ref. 9). The energy levels of the key states are as follows; $^1D^*$ (1.97 eV), $^1H^*$ (1.95 eV), $D^+$—$H^-$—I (1.59 eV), D—$H^+$—$I^-$ (2.05 eV), and $D^+$—H—$I^-$ (1.48 eV), thereby allowing a sequential ET relay of eq. 4. The fluorescence intensity of H—I dyad is identical to that of H alone, indicating that there is no CS in the $^1H^*$—I subunit. On the other hand, a strong fluorescence quenching in the D—H subunit is observed. The transient absorption spectrum of D—H taken for excitation at 618 nm at 20-ps delay time shows immediate build-up of the absorption bands at 670 and 870 nm that are characteristic of $D^+$ and $H^-$, respectively. Fig. 1 displays the transient absorption spectra of D—H—I from 20-ps to 5-ns delay times. The spectrum at 20-ps delay time is essentially the same as that of D—H. These spectra clearly indicate a high yield formation of $D^+$—$H^-$—I and $D^+$—$H^-$ from D—H—I and D—H, respectively, within 20 ps. Analysis of the kinetic trace of the 870-nm absorption has revealed that $D^+$—$H^-$ decays to the ground state with a time constant of 1.2 ns. In the case of $D^+$—$H^-$—I, the decay of the $H^-$ absorption is much faster with a time constant of 200 ps which is accompanied by a rise of the 715-nm absorption due to $I^-$ with the same 200-ps time constant. These data showed that $D^+$—$H^-$—I undergoes CSH reaction to give $D^+$—H—$I^-$ in competition with CR to the ground state. Eventually the secondary ion-pair $D^+$—H—$I^-$ with a lifetime of 280 ns is produced in 0.8 overall quantum yield. The reaction route leading to $D^+$—H—$I^-$ can be summarized as shown in eq. 4, which is quite analogous to that in RC.

$$^1D^*\text{—H—I} \qquad D\text{—}^1H^*\text{—I} \rightarrow D^+\text{—}H^-\text{—I} \rightarrow D^+\text{—H—}I^- \qquad (4)$$
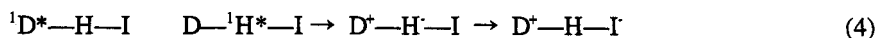
In polar DMF, excitation of D—H leads to the formation of $D^+$—$H^-$ within 10 ps, which rapidly decays to the ground state by CR with a time constant of 50-60 ps. Increase of CR rate in polar DMF is notable. Since very poor solubility of D—H—I in DMF hampered its transient absorption measurement, we have compared the excited-state dynamics of analogous D—H—I triad bearing a 4,4'-biphenyl bridge between D and H in THF and DMF. The ET dynamics are nearly the same in the both solvents, while the overall quantum yield for the formation of the secondary ion pair is ca. 0.79 in THF and only 0.1 in DMF. The main reason for the reduction of the quantum yield is a rapid CR reaction of $D^+$—$H^-$—I $\rightarrow$ D—H—I in polar DMF solution. A polar environment is of course favorable for ET-process in lowering the energy level of charge separated ion-pair states. But it often accelerates the energy wasteful CR reaction with concomitant decrease of the overall CS quantum yield as observed in the present system. This kinetic aspect may be quite common and should be taken into account in future design of more elaborated photosynthetic model systems.

**D—Z—I** First, the ET dynamics in DMF are described. In DMF, the energy levels are as follows; D—$^1Z^*$—I (2.13 eV), $^1D^*$—Z—I (1.93 eV), $D^+$—$Z^-$—I (1.79 eV), and $D^+$—Z—$I^-$ (1.19 eV), being favorable for the sequential ET relay of $^1D^*$—Z—I $\rightarrow$ $D^+$—$Z^-$—I $\rightarrow$ $D^+$—Z—$I^-$. The $^1Z^*$—I subunit can undergo CS to give $Z^+$—$I^-$ (1.75 eV) with a rate of $1.4 \times 10^9$ s$^{-1}$. However, the energy transfer from D—$^1Z^*$ to

$^1$D*—Z is much faster ($1.7 \times 10^{11}$ s$^{-1}$) than this CS. Therefore, all the excitation energies absorbed by the D and Z subunits are preferentially collected at the D subunit. The transient absorption spectra revealed a sequential ET relay of $^1$D*—Z—I → D$^+$—Z$^-$—I → D$^+$—Z—I$^-$ which is similar to that observed for D—H—I. Initially the absorption bands at 440 and 910 nm due to Z$^-$ rise and decay with time constants of 70 and 130 ps, respectively, which is accompanied by the rise of the absorption band of I$^-$ at 715 nm. In summary, this triad provides D$^+$—Z—I$^-$ in 0.4 quantum yield via the reaction sequence of eq. 5 and the lifetime of D$^+$—Z—I$^-$ is 310 ns.

$$D—{}^1Z*—I \rightarrow {}^1D*—Z—I \rightarrow D^+—Z^-—I \rightarrow D^+—Z—I^- \qquad (5)$$
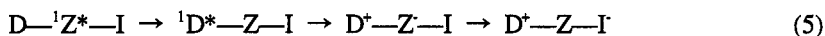
In the less polar THF, the energy levels are as follows; D—$^1$Z*—I (2.13 eV), $^1$D*—Z—I (1.97 eV), D$^+$—Z$^-$—I (1.99 eV), D—Z$^+$—I$^-$ (1.88 eV), and D$^+$—Z—I$^-$ (1.48 eV). In contrast to the situation in DMF, the energy levels of $^1$D*—Z—I and D$^+$—Z$^-$—I are nearly the same. Here again, the energy transfer from D—$^1$Z*—I → $^1$D*—Z—I is much faster ($1.7 \times 10^{11}$ s$^{-1}$) than the charge separation of D—$^1$Z*—I → D—Z$^+$—I$^-$ ($1.2 \times 10^9$ s$^{-1}$). The transient absorption spectra of D—Z dyad taken for excitation at 625 nm have revealed that $^1$D*—Z decays essentially the same manner as that of the reference $^1$D*. We could not find any additional decaying pathway available for the $^1$D*—Z subunit. In particular, the charge separated species D$^+$—Z$^-$ was not detected. On the other hand, $^1$D*—Z—I provides D$^+$—Z—I$^-$ with a time constant of ca. 500 ps. Interestingly, Z$^-$ species could not be detected by the ps transient absorption spectroscopy. A possible mechanism may be that there is an equilibrium between $^1$D*—Z—I and D$^+$—Z$^-$—I, and the latter is effectively trapped by CSH reaction to give D$^+$—Z—I$^-$ as reported for the related zinc chlorin (ZC)—Z—I triad in the same solvent (ref. 10). In this pre-equilibrium case, the decay of $^1$ZC* should be somehow accelerated through this equilibrium and its fluorescence decay becomes biexponential, reflecting the presence of re-generation of the excited state. However, such phenomena were not observed in D—Z—I.
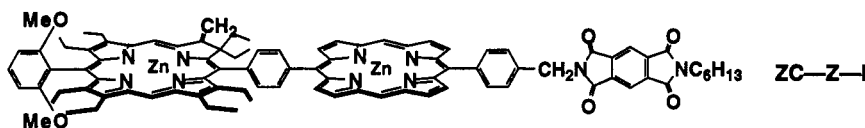


Alternatively, one may envision a direct, long-distance electron transfer via a superexchange mechanism. In this case, the intermediate ion-pair state can be used as a virtual state in the superexchange mechanism. According to the formalism developed for the superexchange mechanism (ref. 11), the electronic matrix element, $V$s, for the superexchange interaction between states i, m, and n, where i and n are the initial and final states and m is the virtual state, is given by eq. 6,

$$V_s = V_{mi}V_{nm}/\Delta E_{mi} \qquad (6)$$

where $V_{mi}$ and $V_{nm}$ are the respective electronic interaction matrix elements between the states i and m, and m and n, and $\Delta E_{mi}$ is the energy difference between the states i and m. In this case, i = $^1$D*—Z—I, m = D$^+$—Z$^-$—I, and n = D$^+$—Z—I$^-$, respectively. In THF, the energy level of D$^+$—Z$^-$—I is estimated to be slightly higher than that of $^1$D*—Z—I and small $\Delta E_{mi}$ may encourage the superexchange ET. But discrimination of the two mechanism seems to be difficult as in the case of RC.

$$D—{}^1Z*—I \rightarrow {}^1D*—Z—I \rightarrow D^+—Z—I^- \qquad (7)$$
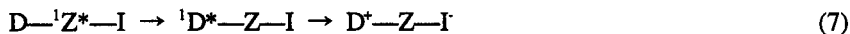
Through these studies, one may conclude that supramolecular porphyrin arrays appropriately designed in respects of geometry and energetics can operate as one expects. The rational molecular design, however, needs a very detailed knowledge of all the effects of a given structural perturbation on the rates of energy- and electron-transfer reactions and on the reaction mechanism as well. Environmental effects that are provided by the surrounding proteins and are considered to play key roles in biological ET should be incorporated into future more elaborated model systems.

## Acknowledgment

## References

1. J. Deisenhofer, O. Epp, K. Miki, H. Michel and H. Huber, *J. Mol. Biol.* **180**, 385 (1984).

2. M. R. Wasielewski, *Chem. Rev.* **92**, 435 (1992).

3. K. Maruyama, A. Osuka and N. Mataga, *Pure Appl. Chem.* **66**, 867 (1994).

4. A. Osuka, S. Nakajima, T. Nagata, K. Maruyama and K. Toriumi, *Angew. Chem. Int. Ed. Engl.* **30**, 582 (1991).

5. A. Osuka, S. Nakajima, K. Maruyama, N. Mataga, T. Asahi, I. Yamazaki, Y. Nishimura, T. Ohno and K. Nozaki , *J. Am. Chem. Soc.* **115**, 4577 (1993).

6. H. Nakaumura, M. Terazima, N. Hirota, S. Nakajima and A. Osuka, *Bull. Chem. Soc. Jpn.* **68**, 2193 (1995).

7. A. Osuka, H. Yamada, K. Maruyama, T. Ohno, K. Nozaki, T. Okada, Y. Tanaka and N. Mataga, *Chem. Lett.*, 591 (1995).

8. A. Osuka, T. Okada, S. Taniguchi, K. Nozaki, T. Ohno and N. Mataga, *Tetrahedron Lett.* **36**, 5781 (1995).

9. A. Osuka, S. Nakajima, T. Okada, S. Taniguchi, K. Nozaki, T. Ohno, I. Yamazaki, Y. Nishimura and N. Mataga, *Angew. Chem., Int. Ed. Engl.* **35**, 92 (1996).

10. A. Osuka, S. Marumo, N. Mataga, S. Taniguchi, T. Okada, I. Yamazaki, Y. Nishimura, T. Ohno and K. Nozaki, *J. Am. Chem. Soc.* **118**, 155 (1996).

11. Y. Won and R. A. Friesner, *Biochim. Biophys. Acta* **935**, 9 (1988).